8-1991

Analysis of Vibration Eigenfrequencies of a Thin Plate by the Keller-Rubinow Wave Method .1. Clamped Boundary-Conditions with Rectangular or Circular Geometry

G. Chen

Matt Coleman
Fairfield University, mcoleman@fairfield.edu

J.X. Zhou

Published Citation

G. Chen, M. P. Coleman, and J.X. Zhou. *Analysis of Vibration Eigenfrequencies of a Thin Plate by the Keller-Rubinow Wave Method .1. Clamped Boundary-Conditions with Rectangular or Circular Geometry,* Siam Journal on Applied Mathematics. 51(4), 967-983.

SIAM J. APPL. MATH.
Vol. 51, No. 4, pp. 967-983, August 1991

ANALYSIS OF VIBRATION EIGENFREQUENCIES OF A THIN PLATE BY THE KELLER–RUBINOW WAVE METHOD I: CLAMPED BOUNDARY CONDITIONS WITH RECTANGULAR OR CIRCULAR GEOMETRY*

GOONG CHEN†, MATTHEW P. COLEMAN‡, AND JIANXIN ZHOU§

Abstract. The wave method of Keller and Rubinow [*Ann. Physics*, 9 (1960), p. 24–75] is extended to the *biharmonic* eigenvalue problem with rectangular or circular geometry and clamped boundary conditions. First, it is noted from the clues of computer graphics that mode shapes of a clamped circular plate and those of a circular membrane look very similar to each other. This suggests that *plate and membrane should have very similar vibration behavior* and leads to the *assumption* that *the covering space of a rectangular plate is still a torus.* By adding several *waves on the boundary*, approximate eigenfrequency equations are derived. Their solutions are shown to agree remarkably with numerical solutions obtained by the Legendre-tau spectral method here and by the finite-element method elsewhere at all frequency ranges. The same idea is also applied to the circular plate and yields excellent agreement between the exact values of eigenfrequencies and the asymptotic solutions.

Key words. thin plate, wave method, eigenfrequency, wavenumber, spectral and finite-element methods

AMS(MOS) subject classifications. 35P20, 73D30, 73K12

1. Introduction and motivation. Consider a vibrating thin Kirchhoff *plate* eigenvalue problem subject to clamped boundary conditions

$$\Delta^2\phi(x)-\lambda^2\phi(x)=0, \quad x\in\Omega \quad (\Delta^2 \text{ is the biharmonic operator}),$$

$$\phi(x)=\frac{\partial\phi}{\partial n}(x)=0 \quad \text{on } \partial\Omega. \tag{1.1}$$

In the literature on plates, it is known that for (1.1) on a rectangular domain, for example,

$$\Omega=\{(x_1, x_2)\,|\,0<x_1<a, 0<x_2<b\}, \tag{1.2}$$

the variables x_1 and x_2 are *not separable* (cf., e.g., the classic of Courant and Hilber [7, p. 307]). (This is perhaps the most important and best-known example of boundary value problems for which separation of variables does not work.)

An analogous problem is the vibrating *membrane* eigenvalue problem subject to the fixed boundary condition

$$\Delta\phi(x)+\lambda^2\phi(x)=0, \qquad x\in\Omega,$$

$$\phi(x)=0 \quad \text{on } \partial\Omega. \tag{1.3}$$

We have computed and plotted a set of eigenfunctions for the plate and the membrane on a circular domain using the separation of variables solutions. We have found a striking feature shown in those figures that the *profiles of the plate's and*

* Received by the editors September 6, 1989; accepted for publication (in revised form) July 16, 1990.

† Departments of Mathematics and Aerospace Engineering, Texas A&M University, College Station, Texas 77843. The research of this author was supported in part by Air Force Office of Scientific Research grant 87-0334 and National Science Foundation grant DMS 87-18510.

‡ Department of Mathematics and Computer Science, Fairfield University, Fairfield, Connecticut 06430.

§ Department of Mathematics, Texas A&M University, College Station, Texas 77843. The research of this author was supported in part by Air Force Office of Scientific Research grant 87-0334 and National Science Foundation grant DMS 87-18510.

membrane's eigenfunctions are essentially similar, without ever missing the proper sequential order (at least for the first ten modes seen by us). The only visual difference is that the plate's eigenmodes are *flatter near the boundary* in order to meet the additional boundary restraint $\partial\phi/\partial n = 0$. The reader can compare the resemblance and difference of the tenth eigenmode of the plate and the membrane in Figs. 1(a) and 1(b). The computer graphics suggest that *wave propagation on a plate and membrane is essentially similar*, and that the wave method developed by Keller and Rubinow in [11] is likely to be applicable to the plate with some adaptation. This motivates the study in this paper. As it turns out, the adaptation to be made is just to *add several waves propagating along the boundary but evanescent in the orthogonal directions*, extremely similar to the beam case treated by us in [3].

We plan to write a series of papers on the topic of the wave method for the plate equation. Here, in Part I, we will focus on the case of rectangular and circular geometries with clamped boundary conditions. For the rectangular plate, we will

(1) Use the Keller–Rubinow wave method to derive the asymptotic transcendental equations for the eigenfrequencies and therefrom compute numerical solutions.

(2) Use the Legendre spectral method to directly compute the spectrum of a clamped square plate. The scientific computation was carried out on the ETA 10 Supercomputer at the John von Neumann Center at Princeton, New Jersey, with parallel and vectorized codes and algorithms, enabling us to obtain larger solution data than what is available in the literature for asymptotic comparisons.

For the circular plate, we add waves propagating on the circumference, derive the reflection relation, and determine the asymptotic formula, generalizing Keller and Rubinow's approach in [11] to a plate.

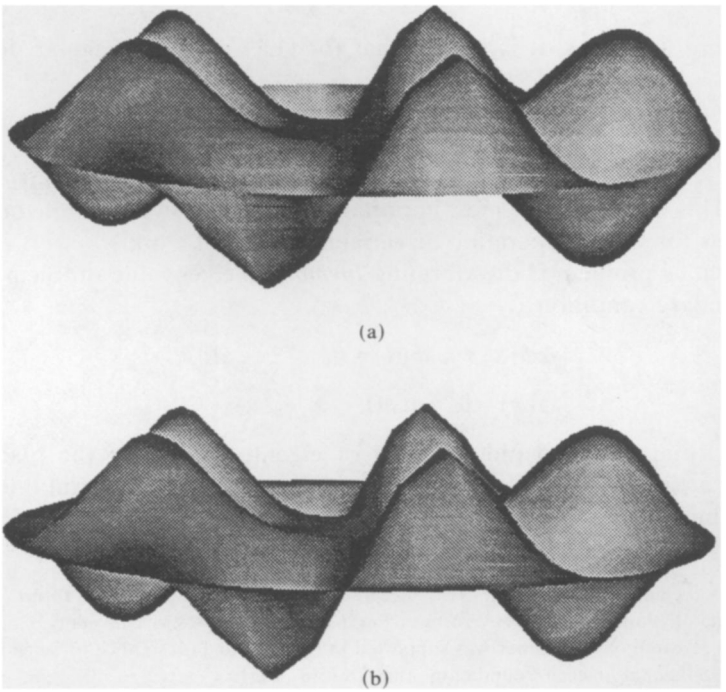

FIG. 1. (a) *The tenth eigenmode* $J_5(8.77148r)\exp(\pm i5\theta)$, *real part, of circular membrane* (*multiplicity* 2). (b) *The tenth eigenmode* $[a_1J_5(9.52570r)+a_2J_5(i9.52570r)]\exp(\pm i5\theta)$ *real part, of circular plate* (*multiplicity* 2).

The comparison of our theoretical and numerical results shows excellent agreement even at the lowest eigenfrequency and essentially validates the Keller-Rubinow wave method for a plate.

In subsequent parts of this series of papers, we would like to

(i) Study the plate equation subject to higher-order boundary conditions (hinged, roller-supported, free, etc.);

(ii) Compare the spectral data from laboratory mechanical experiments with the mathematical data; and

(iii) Show the convergence of a plate to a beam when the width of the plate is reduced.

2. The Keller–Rubinow wave method and its adaptation to the plate. In [11], Keller and Rubinow used ideas from wave propagation to derive eigenvalue estimates for the Laplacian. The mathematical rigor of their approach is justified in the asymptotic sense by Maslov (see Maslov and Fedoriuk [15]). It is understood that the theory given in [15] is valid even for higher-order equations (and with variable coefficients), including the plate equation (1.1). But to apply the full power of Maslov-Fedoriuk [15] is impractical herein because it involves calculating trajectories of Hamilton-Jacobi equations, which is generally rather complicated, as indicated, e.g., in a more recent survey article [5]. It is much easier for us to directly invoke the physical insights as provided by Keller-Rubinow [11] for the problem of our concern here.

Let us give a quick review of Keller and Rubinow's ideas for the Helmholtz equation (1.3). Let $\lambda = k$, the wavenumber. According to the geometrical theory of optics (GTO) [12], [13] when $|k|$ is large, ϕ can be represented by a geometrical optics expansion

$$\begin{aligned}\phi(x) &= \sum_{j=1}^{N} e^{ikS_j(x)}\left[\sum_{p=0}^{\infty}\frac{A_{j,p}(x)}{(ik)^p}\right] \\ &= \sum_{j=1}^{N} e^{ikS_j(x)}\left[A_{j,0}(x)+\mathcal{O}\left(\frac{1}{k}\right)\right], \qquad x\in\Omega,\end{aligned} \tag{2.1}$$

where it is assumed that there are N waves propagating in Ω. Each wave has phase S_j and (dominant) amplitude $A_{j,0}$. Substituting (2.1) into (1.3) and equating to zero the coefficients of k^2 and k, we obtain

$$|\nabla S_j|^2 = 1 \quad \text{(the eiconal equation)}, \tag{2.2}$$

$$2\nabla S_j\cdot\nabla A_{j,0} + A_{j,0}\Delta S_j = 0 \quad \text{(the transport equation)} \tag{2.3}$$

for $j = 1, 2, \cdots, N$. The transport equation (2.3) is an ordinary differential equation along a ray (which are orthogonal trajectories to the surfaces $S_j = \text{const.}$) and can be integrated (up to a caustic), giving the amplitude $A_{j,0}(x)$. When a wave $\exp[ikS_j(x)]\cdot[A_{j,0}(x)+\mathcal{O}(1/k)]$ hits the boundary, it gives rise to a *reflected wave* $\exp[ikS_j'(x)]\cdot[A_{j',0}(x)+\mathcal{O}(1/k)]$. A similar change of waves also occurs when a wave is converging to a *caustic*, giving rise to another wave diverging from the caustic. Let us now trace a ray of any wave in the direction of increasing arclength; taking into account the reflection at boundary or the passing of a caustic, the ray continues as a sequence of rays of other waves. Since there are, by assumption, only a finite number N of waves in the solution, one of the waves in this sequence must *recur*. To form an eigenmode ϕ, *resonance must occur*, i.e., the wave that recurs must be *in phase with itself*, that is to say, the overall phase difference due to the changes of S_j and $A_{j,0}$ must be an integral multiple of 2π. This is expressed [11, p. 29, (18)] by

$$k(\delta S_j) + \delta(\arg A_{j,0}) = 2\pi n_j, \qquad j = 1, \cdots, N, \quad n_j\in\mathbb{Z}, \tag{2.4}$$

where δS_j and $\delta(\arg A_{j,0})$ denote, respectively, the changes of S_j and the argument of the complex amplitude A_j.

In [11], Keller and Rubinow further used the important topological concept of a *covering space* to resolve the difficulty of the *multivaluedness* of the S_j by regarding them as branches of a single function S. The covering space is multisheeted, just like a Riemann surface in complex variable theory. The various sheets are replicas of the domain Ω, which may be bounded internally by caustics. The sheets corresponding to ∇S_{j1} and ∇S_{j2} are joined together along the part of the caustic or the boundary where $S_{j1} = S_{j2}$, the places where the wave j_1 gives rise to the wave j_2 by reflection or by passing through a caustic. Similarly, $A_{j,0}$ are considered as branches of a single function A defined on the covering space. Assume that the *fundamental group* of the covering space contains q linearly independent closed curves C_j, $j = 1, 2, \cdots, q$. Then the condition (2.4) can be rewritten as [11, p. 30, (20)]

$$k \oint_{C_j} \nabla S \cdot d\sigma + \sum \delta(\arg A) = 2\pi n_j, \qquad j = 1, 2, \cdots, q, \quad n_j \in \mathbb{Z}. \tag{2.5}$$

We return to the plate equation. Letting $\lambda = k^2$ in the first equation of (1.1),

$$(\Delta^2 - k^4)\phi(x) = 0, \tag{2.6}$$

we have

$$(\Delta - k^2)(\Delta + k^2)\phi(x) = 0,$$

so

$$\phi(x) = \phi_1(x) + \phi_2(x),$$

where ϕ_1 and ϕ_2 satisfy

$$(\Delta + k^2)\phi_1(x) = 0, \tag{2.7}$$

$$(\Delta - k^2)\phi_2(x) = 0. \tag{2.8}$$

Equation (2.7) is a Helmholtz equation so the ansatz (2.1) in GTO applies to ϕ_1. However, for (2.8), (2.1) is not directly applicable and the solutions have very different behavior. For example, it may contain (the so-called overdamped) solutions such as

$$\phi_2(x) = A \exp(-k(\eta_1 x_1 + \eta_2 x_2)), \qquad A \in \mathbb{C}, \quad \eta_1, \eta_2 \in \mathbb{R}, \quad \eta_1^2 + \eta_2^2 = 1, \tag{2.9}$$

which are not oscillatory at all. According to our approach devised herein, such entirely overdamped modes will not play any role in the plate wave propagation. The modes of (2.8) that do participate in the plate wave propagation are the *special* type of *waves*—those that are *oscillary in one axial direction* but *overdamped in the (internal) orthogonal direction.* In the case of rectangular and circular geometries, these axial directions can be aligned with the boundary (curvilinear) coordinate axes, which critically facilitates the tractability of the problem using our approach. An anonymous reviewer pointed out to us that an adapted asymptotic expansion method, developed by Cohen et al. in [4] and [5] (see also the reference therein) can be applied to (2.8) (cf. particularly § 5 in [4]), where the coefficient a in [4, (5.2.1)] is negative, making $\lambda^2 a$ therein correspond to $-k^2$ in (2.8). We are hoping to use these references to rigorize our arguments in this paper and to report the finding in the future.

Let us proceed to explain how the method works and to provide the numerical validation in the next few sections.

3. The eigenfrequency analysis of the rectangular plate. We consider (1.1) with rectangular geometry (1.2). The four sides of Ω are denoted as S_j, $j = 1, 2, 3, 4$ (see

Fig. 2I). On $\partial\Omega$, the clamped conditions in (1.1) are in effect. The analysis of asymptotic distribution of eigenvalues of *self-adjoint*, partial differential, boundary value problems *on a rectangular domain*, including our problem under study in this section, was considered Bolotin in [2]. (This was pointed out to us by a second reviewer, after our investigations in §§ 2 and 3 were complete.) The main idea therein is close to a separation of variables method. It does not cover the cases of *different geometries* (circular, elliptical, etc.) or *nonself-adjoint problems.* Our approach here allows more ready extension to other geometries (cf. § 5) and is probably more aptly generalizable to *dissipative boundary conditions* (which are *nonself-adjoint*). Nevertheless, we have found the work of Bolotin [2] interesting and useful, and hope to be able to incorporate it into the wave method to treat a larger class of problems on rectangular domains.

The greatest advantage of using the wave method for rectangular geometry is that *wave functions* are easy to determine. Let

$$k = \text{the wavenumber} > 0,$$

$$\left.\begin{aligned}\eta_1 &= \cos\theta\\ \eta_2 &= \sin\theta\end{aligned}\right\}\ \theta \text{ is the angle formed by the ray with the } x_1\text{-axis.} \tag{3.1}$$

Then it is known from [11] that for the Helmholtz equation (2.7) there are four wave functions as given in Table 1.

For the plate equation (2.6), there are eight additional waves corresponding to solutions of (2.8) propagating along the boundary axes, two on each side (see Table 2).

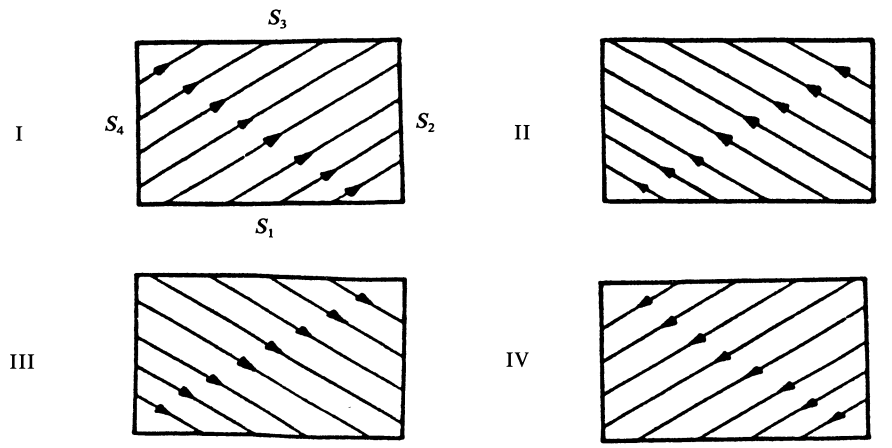

FIG. 2. *The four waves* I–IV *propagating on the interior of the rectangular domain.*

TABLE 1

The four wave functions of the Helmholtz equation (2.7). *Note that the time-dependence is* e^{ikt} *for the wave equation and* e^{ik^2t} *for the plate equation.*

Wave	*Wave functions*
I	$\exp(-ik(\eta_1 x_1 + \eta_2 x_2))$
II	$\exp(ik(\eta_1 x_1 - \eta_2 x_2))$
III	$\exp(ik(\eta_1 x_1 + \eta_2 x_2))$
IV	$\exp(-ik(\eta_1 x_1 - \eta_2 x_2))$

TABLE 2

The eight physically admissible wave functions of (2.8) *that propagate along the boundary axes but are evanescent in the interior orthogonal direction. Note that the time-dependence is* e^{ik^2t} *for the plate equation. See Fig.* 3.

Wave	Wave functions
V	$\exp(-k(\sqrt{1+\eta_2^2}\,x_1+i\eta_2x_2))$
VI	$\exp(-k[i\eta_1x_1+\sqrt{1+\eta_1^2}\,(b-x_2)])$
VII	$\exp(k[-\sqrt{1+\eta_2^2}\,(a-x_1)+i\eta_2x_2])$
VIII	$\exp(k(i\eta_1x_1-\sqrt{1+\eta_1^2}\,x_2))$
IX	$\exp(k(-\sqrt{1+\eta_2^2}\,x_1+i\eta_2x_2))$
X	$\exp(-k(i\eta_1x_1+\sqrt{1+\eta_1^2}\,x_2))$
XI	$\exp(-[\sqrt{1+\eta_2^2}\,(a-x_1)+i\eta_2x_2])$
XII	$\exp(k[i\eta_1x_1-\sqrt{1+\eta_1^2}\,(b-x_2)])$

We remark that (2.7) and (2.8) have more solutions (which are similar to plane waves) than those listed in Tables 1 and 2. Just look at (2.9), which has been ruled out earlier. Other wave forms such as $\exp(k(-i(1+\eta_2^2)^{1/2}x_1-\eta_2x_1))$ and $\exp k(\eta_1x_1-\eta_2x_2))$ (satisfying (2.7) and (2.8), respectively) are also ruled out as *physically inadmissible* either because they are not the usual membrane waves or because they are exponentially growing in at least one of the axial directions.

In the case of the wave equation (1.2), Keller and Rubinow observed that there are *four normal congruences of rays* (cf. Table 2) from which all the waves arising by successive reflections are still of these four normal congruences. The *covering space* therefore is deduced to be a *torus* (cf. [11, p. 58]). By comparing the wave functions I–IV in Tables 1 and 2, we see that they propagate along the same directions. The only difference is that these four waves on plate are *dispersive, for the time-dependence is* e^{ik^2t} *instead of* e^{ikt}, so waves with larger wavenumber k travel faster. The role of the eight remaining physically admissible waves V–XII in Table 2 should be only to modify the wave profile at the boundary, a viewpoint supported by our understanding derived from Fig. 1. Since the propagation of the four principal waves I–IV can be decomposed into vertical and horizontal directions, it is natural to assume that the covering space of the plate waves is still a torus, just as in [11]. The correctness and usefulness of this assumption will be evidenced by the arguments used by us below, and by comparing the outcome with the numerical solutions in the next sections, which are meant to be a validation to this assumption.

Consider the following four waves propagating in Ω:

$$\begin{aligned}\psi_v(x,t)\equiv{}& A_1\exp(ik[kt-(\eta_1x_1+\eta_2x_2)])+A_2\exp(ik[kt-\eta_1x_1-\eta_2(b-x_2)])\\ &+B\exp(ik(kt-\eta_1x_1)-k\sqrt{1+\eta_1^2}\,x_2)\\ &+C\exp(ik(kt-\eta_1x_1)-k\sqrt{1+\eta_1^2}\,(b-x_2)),\qquad k>0\end{aligned}\tag{3.2}$$

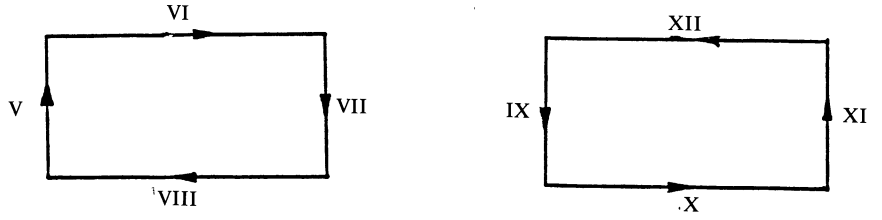

FIG. 3. *The eight waves* V–XII *propagating on the boundary of a rectangular plate.*

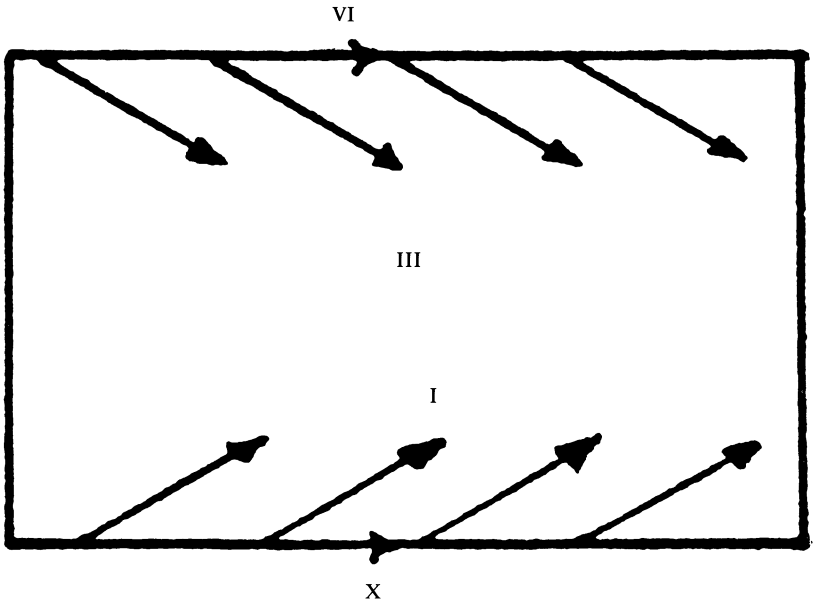

FIG. 4. *The four waves in* ψ_v *of* (3.2).

(cf. Fig. 4). Note that these waves (with amplitudes) A_1, A_2, B, and C are, respectively, waves of type I, II, X, and VI in Tables 1 and 2. The wave pairs A_1, B and A_2, C are selected in order to match the boundary conditions at, respectively, the bottom edge S_1 and the top edge S_3, and the wave pair A_1, A_2 are reflections of each other at the top and bottom edges. Now applying the clamped conditions at the bottom edge $x_2 = 0$

$$w(x_1, 0, t) = 0, \qquad \frac{\partial}{\partial x_2} w(x_1, 0, t) = 0$$

to $\psi_v(x, t)$, we obtain

$$\begin{aligned} &A_1 + e^{-ikb\eta_2} A_2 + B + \exp(-kb\sqrt{1+\eta_1^2})C = 0, \\ &-ik\eta_2 A_1 + ik\eta_2\, e^{-ikb\eta_2} A_2 - k\sqrt{1+\eta_1^2}\, B + k\sqrt{1+\eta_1^2} \exp(-kb\sqrt{1+\eta_1^2})C = 0. \end{aligned} \tag{3.3}$$

Similarly, applying the clamped conditions at the top edge $x_2 = b$, we obtain

$$\begin{aligned} &e^{-ikb\eta_2} A_1 + A_2 + \exp(-kb\sqrt{1+\eta_1^2})B + C = 0, \\ &-ik\eta_2\, e^{-ikb\eta_2} A_1 + ik\eta_2 A_2 - k\sqrt{1+\eta_1^2} \exp(-kb\sqrt{1+\eta_1^2})B + k\sqrt{1+\eta_1^2}\, C = 0. \end{aligned} \tag{3.4}$$

Examine (3.3) first. When k is large, the coefficients of C in two equations are exponentially small as compared to A_1, A_2, and B, so we discard C and obtain two approximate equations

$$\begin{aligned} &A_1 + e^{-ikb\eta_2} A_2 + B = 0, \\ &-ik\eta_2 A_1 + ik\eta_2\, e^{-ikb\eta_2} A_2 - k\sqrt{1+\eta_1^2}\, B = 0. \end{aligned} \tag{3.3}'$$

Similarly, in (3.4), the coefficients of B are exponentially small, and by discarding B we obtain the approximate equations

$$\begin{aligned} &e^{-ikb\eta_2}A_1 + A_2 + C = 0, \\ &-ik\eta_2\, e^{-ikb\eta_2}A_1 + ik\eta_2 A_2 + k\sqrt{1+\eta_1^2}\, C = 0. \end{aligned} \tag{3.4}'$$

We eliminate B in (3.3)', obtaining the *reflection relation*

$$A_1 = -\left(\frac{\sqrt{1+\eta_1^2}+i\eta_2}{\sqrt{1+\eta_1^2}-i\eta_2}\right) e^{-ikb\eta_2}A_2, \tag{3.5}$$

where as far as the bottom edge S_1 is concerned, $A_2\, e^{-ikb\eta_2}$ is the amplitude of the incident wave and A_1 is the amplitude of the reflected wave. Similarly, if we eliminate C in (3.4)', we obtain the reflection relation

$$A_2 = -\left(\frac{\sqrt{1+\eta_1^2}+i\eta_2}{\sqrt{1+\eta_1^2}-i\eta_2}\right) e^{-ikb\eta_2}A_1, \tag{3.6}$$

where for the top edge S_3 the roles of incident and reflected waves have exchanged between A_1 and A_2. From (3.5) and (3.6), we obtain

$$\left(\frac{\sqrt{1+\eta_1^2}+i\eta_2}{\sqrt{1+\eta_1^2}-i\eta_2}\right)^2 e^{-2ikb\eta_2} = 1, \tag{3.7}$$

and consequently

$$2\arg\left(\frac{\sqrt{1+\eta_1^2}-i\eta_2}{\sqrt{1+\eta_1^2}+i\eta_2}\right) + 2kb\eta_2 = 2m\pi, \qquad m = 1, 2, 3, \cdots. \tag{3.8}$$

The relations (3.3), (3.4), (3.3)', (3.4)', and (3.8) have taken care of the *vertical* motion of the plate waves. *Equation* (3.8) *is essentially* (2.5) *for the vertical path in the fundamental group of the torus.*

Next, we consider the *horizontal* motion of waves. Write

$$\begin{aligned} \psi_h(x, t) = {} & \tilde{A}_1 \exp\left(ik[kt - (\eta_1 x_1 + \eta_2 x_2)]\right) + \tilde{A}_2 \exp\left(ik[kt - \eta_1(a - x_1) - \eta_2 x_2]\right) \\ & + \tilde{B} \exp(ik[kt - \eta_2 x_2] - k\sqrt{1+\eta_2^2}\, x_1) \\ & + \tilde{C} \exp(ik(kt - \eta_2 x_2] - k\sqrt{1+\eta_2^2}\,(a - x_1)) \end{aligned} \tag{3.9}$$

similarly as before. These waves are depicted in Fig. 5. Applying the clamped conditions at the left and right edges S_2 and S_4 on the rectangle and repeating the calculations,

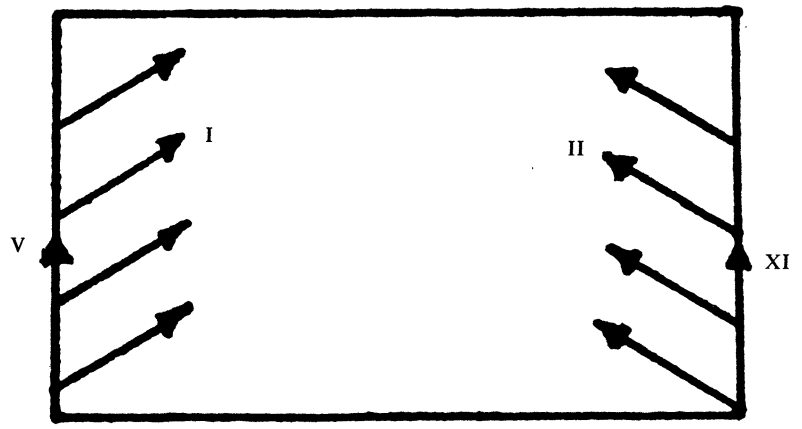

FIG. 5. *The four waves in* ψ_h *of* (3.9).

we obtain similarly

$$2\arg\left(\frac{\sqrt{1+\eta_2^2}-i\eta_1}{\sqrt{1+\eta_2^2}+i\eta_1}\right)+2ka\eta_1=2l\pi, \qquad l=1,2,3,\cdots. \tag{3.10}$$

This is essentially the second equation of (2.5) *for the horizontal path in the fundamental group of the torus.* Therefore we have obtained a system of three nonlinear equations for k, η_1, η_2:

$$\begin{aligned} &2\arg\left(\frac{\sqrt{1+\eta_2^2}-i\eta_1}{\sqrt{1+\eta_2^2}+i\eta_1}\right)+2ka\eta_1=2l\pi, \qquad l=1,2,3,\cdots,\\ &2\arg\left(\frac{\sqrt{1+\eta_1^2}-i\eta_2}{\sqrt{1+\eta_1^2}+i\eta_2}\right)+2kb\eta_2=2m\pi, \qquad m=1,2,3,\cdots,\\ &\eta_1^2+\eta_2^2=1, \end{aligned} \tag{3.11}$$

valid when k is large. The two integers l and m appearing in (3.11) will be aptly called, respectively, the *wave cell numbers* in the x_1 and x_2 directions. They are related to the lattice numbers in the nodal line patterns of the eigenmodes. An easy consequence of this is that $\lambda=k^2$ (cf. (1.1) for λ), the eigenfrequency, should satisfy

$$\begin{aligned} &\frac{\lambda}{\left(\frac{l\pi}{a}\right)^2+\left(\frac{m\pi}{b}\right)^2}\\ &=\frac{k^2}{\left(\frac{l\pi}{a}\right)^2+\left(\frac{m\pi}{b}\right)^2}\\ &=\frac{\frac{1}{a^2}\left[l\pi-\arg\left(\frac{\sqrt{1+\eta_1^2}-i\eta_2}{\sqrt{1+\eta_1^2}+i\eta_2}\right)\right]^2+\frac{1}{b^2}\left[m\pi-\arg\left(\frac{\sqrt{1+\eta_2^2}-i\eta_1}{\sqrt{1+\eta_2^2}+i\eta_1}\right)\right]^2}{\left(\frac{l\pi}{a}\right)^2+\left(\frac{m\pi}{b}\right)^2}\to 1, \end{aligned}$$

as l, $m\to\infty$. This is in contrast to

$$\frac{\lambda}{[(\lambda\pi/a)^2+(m\pi/b)^2]^{1/2}}=1$$

for a rectangular membrane (cf. the λ in (1.3) for a rectangular domain (1.2)).

The nonlinear system (3.11) can be solved numerically as follows. Let

$$\eta_1=\cos\theta, \qquad \eta_2=\sin\theta \tag{3.12}$$

from (3.1). Multiply the first equation in (3.11) by η_2/a and the second by η_1/b and subtract. We obtain a nonlinear equation in θ:

$$\begin{aligned} &\frac{\sin\theta}{a}\arg\left(\frac{\sqrt{1+\sin^2\theta}-i\cos\theta}{\sqrt{1+\sin^2\theta}+i\cos\theta}\right)-\frac{\cos\theta}{b}\arg\left(\frac{\sqrt{1+\cos^2\theta}-i\sin\theta}{\sqrt{1+\cos^2\theta}+i\sin\theta}\right)\\ &\quad=\left(\frac{l}{a}\sin\theta-\frac{m}{b}\cos\theta\right)\pi. \end{aligned}$$

From this equation, we approximate θ by a standard Newton method. From (3.12), we obtain η_1 and η_1. Then k can be obtained from either the first or the second equation in (3.11).

For the case of a square, $a=b=1$, solutions to k and η_1 in (3.12) (computed by the numerical procedure above) can be found in Table 3 in § 4, to be compared with the k's obtained by purely numerical procedures such as the spectral method.

4. The Legendre-tau spectral method for computing eigenfrequencies of a rectangular plate, and comparison with the wave method. There are numerical data of eigenfrequencies of a *square* plate available in the literature (see, e.g., Bauer and Reiss [1] and Hackbusch and Hofmann [10]). They were computed by using the finite-element method. Hackbusch and Hofmann's paper [10] lists the first 46 (counting up to multiplicity) eigenfrequencies. In order to have a larger set of data in the asymptotic range for comparison, we use a highly accurate Legendre-tau spectral method computer package developed by Coleman in his Ph.D. thesis directed by Chen at the Pennsylvania State University. In the software, parallel and vectorized algorithms and codes were adopted to take advantage of the ETA 10 Supercomputer architecture at the John von Neumann Center in Princeton, New Jersey. Since the algorithms and the main body of the computer program are available in Coleman's dissertation [6], in what follows we will only give a brief sketch of the discretization algorithm.

Let

$$\Phi(x_1, x_2) = \phi\left(\frac{a}{2}(x_1+1), \frac{b}{2}(x_2+1)\right), \qquad -1 < x_1\ ,\ x_2 < 1,$$

where ϕ is the eigenfunction satisfying (1.5) and the clamped conditions on a rectangle (1.6). Thus Φ satisfies

$$\frac{16}{a^4}\frac{\partial^4}{\partial x_1^4}\Phi(x_1, x_2) + \frac{32}{a^2b^2}\frac{\partial^4}{\partial x_1^2 \partial x_2^2}\Phi(x_1, x_2) + \frac{16}{b^4}\frac{\partial^4}{\partial x_2^4}\Phi(x_1, x_2) - \lambda^2\Phi(x_1, x_2) = 0, \tag{4.1}$$

$$\begin{aligned} &\Phi(-1, x_2) = 0, && \Phi_{x_1}(-1, x_2) = 0, \\ &\Phi(1, x_2) = 0, && \Phi_{x_1}(1, x_2) = 0, \\ &\Phi(x_1, -1) = 0, && \Phi_{x_2}(x_1, -1) = 0, \\ &\Phi(x_1, 1) = 0, && \Phi_{x_2}(x_1, 1) = 0. \end{aligned} \tag{4.2}$$

We approximate Φ by

$$\Phi_{N,M}(x_1, x_2) = \sum_{n=0}^{N}\sum_{m=0}^{M} a_{nm}P_n(x_1)P_m(x_2),$$

where $P_n(x)$ is the Legendre polynomial of degree n [9]. Substitute $\Phi_{N,M}$ into (4.1) and compare the coefficients of P_nP_m, yielding

$$\begin{aligned} -\lambda^2 a_{ij} &+ \frac{16}{a^4}\sum_{\substack{q=i+2 \\ q+i \text{ even}}}^{N-2}\ \sum_{\substack{p=q+2 \\ p+q \text{ even}}}^{N}\left(i+\frac{1}{2}\right)\left(q+\frac{1}{2}\right)[q(q+1)-i(i+1)][p(p+1)-q(q+1)]a_{pj} \\ &+ \frac{16}{a^2b^2}\sum_{\substack{p=i+2 \\ p+i \text{ even}}}^{N}\ \sum_{\substack{q=j+2 \\ q+j \text{ even}}}^{M}\left(i+\frac{1}{2}\right)\left(j+\frac{1}{2}\right)[p(p+1)-i(i+1)][q(q+1)-j(j+1)]a_{pq} \\ &+ \frac{16}{b^4}\sum_{\substack{q=j+2 \\ q+j \text{ even}}}^{M-2}\ \sum_{\substack{p=q+2 \\ p+q \text{ even}}}^{M}\left(j+\frac{1}{2}\right)\left(q+\frac{1}{2}\right)[q(q+1)-j(j+1)][p(p+1)-q(q+1)]a_{ip} = 0, \\ &\qquad i = 0, 1, \cdots, N-4, \quad j = 0, 1, \cdots, M-4. \end{aligned}$$

We obtain $(N-3)\times(M-3)$ homogeneous linearly independent equations for the coefficients a_{nm}. Next, substitute $\Phi_{N,M}$ into the eight boundary conditions in (4.2) and utilize the fact that

$$P_n(\pm 1)=(\pm 1)^n, \qquad P_n'(\pm 1)=(\pm 1)^{n-1}\cdot\frac{n(n+1)}{2}$$

to equate coefficients. We will obtain $4N+4M+8$ homogeneous linear equations for the coefficients a_{nm}. Of those $4N+4M+8$ equations, 16 *of them are linearly dependent* of the rest because of the connection conditions at the four corners of the square. So we choose a linearly independent subset of $4N+4M+8-16=4N+4M-8$ of equations. Thus a total of

$$(N-3)\times(M-3)+(4N+4M-8)=(N+1)\times(M+1)$$

homogeneous linear equations are obtained for the $(N+1)\times(M+1)$ unknown coefficients a_{nm}. These equations can be assembled into a matrix system

$$(\lambda^2 X+\lambda Y+Z)\mathbf{v}=0, \tag{4.3}$$

where X, Y, and Z are square matrices of size $[(N+1)\times(M+1)]$ by $[(N+1)\times(M+1)]$, and

$$\mathbf{v}=(a_{00}, a_{01}, \cdots, a_{0M}, a_{10}, a_{11}, \cdots, a_{1M}, \cdots, a_{N0}, a_{N1}, \cdots, a_{NM}).$$

Thus (the true) eigenvalues are approximated by the roots of

$$\det(\lambda^2 X+\lambda Y+Z)=0,$$

which has $2(N+1)\times(M+1)$ roots. In our numerical computations,

$$N=M=20$$

have been used, yielding

$$2(20+1)\cdot(20+1)=882$$

roots. A partial list of them will be given in the next section. Note that the matrices X, Y, and Z in (4.3) commonly lack symmetry (and are not sparse), so the computed eigenfrequencies λ may contain a very small imaginary part, of the order of magnitude at most 10^{-4}.

We now list the solutions obtained by the various methods here in Table 3.

The numerical solutions of eigenfrequencies obtained by the Legendre spectral method manifest high accuracy. They have enabled us to detect that the finite-element eigenfrequency solutions obtained by Hackbusch and Hofmann [10] have actually missed several values near the end. This occurrence is rather customary with finite-element eigenvalue computations according to our own numerical experience.

The high agreement of k between these methods at *all* frequencies is clear and remarkable.

5. Analysis of eigenfrequencies of a circular plate. As noted earlier, the circular geometry for the membrane (1.3) has been treated in [11]. Now we utilize the work therein to treat the circular thin plate.

From [11, pp. 35-36], we know that for the circular membrane, $N=2$ in the asymptotic expansion (2.1), with phase functions

$$S_1(r,\theta)=a_0\left[\theta-\cos^{-1}\left(\frac{a_0}{r}\right)\right]+(r^2-a_0^2)^{1/2},$$

$$S_2(r,\theta)=a_0\left[\theta+\cos^{-1}\left(\frac{a_0}{r}\right)-2\cos^{-1}\left(\frac{a_0}{a}\right)\right]+2(a^2-a_0^2)^{1/2}-(r^2-a_0^2)^{1/2},$$

TABLE 3

Comparison of the wavenumber k obtained by the wave method and the Legendre-tau method.

(l, m) are the wave cell integers, W is the wave method, $L\tau$ is the Legendre-tau method. Compute η_2 by $\eta_2 = \sqrt{1-\eta_1^2}$, and compute the eigenfrequency λ in (1.1) by $\lambda = k^2$. Note that the finite-element solutions in Hackbusch and Hofmann [10] agree with the $L\tau$ solutions herein, but have missed the 44–47 and 49, 50th values. Also observe that after the 83rd value, $L\tau$ slowly begins the loss of accuracy, causing the lack of agreement between itself and the wave method.

#	(l, m)		W	$L\tau$	η_1
1	1	1	5.92384	5.99877	0.707107
2	2	1	8.53827	8.56702	0.896776
3	1	2	8.53827	8.56702	0.442484
4	2	2	10.36673	10.40272	0.707107
5	3	1	11.47295	11.47087	0.949855
6	1	3	11.47295	11.49803	0.312691
7	3	2	12.82134	12.84525	0.833388
8	2	3	12.82134	12.84525	0.552689
9	4	1	14.50385	14.50937	0.970740
10	1	4	14.50385	14.50937	0.240132
11	3	3	14.80961	14.83350	0.707107
12	4	2	15.56268	15.56130	0.895601
13	2	4	15.56268	15.59309	0.444858
14	4	3	17.19588	17.21441	0.800788
15	3	4	17.19588	17.21441	0.598948
16	5	1	17.57638	17.57562	0.980916
17	1	5	17.57638	17.58306	0.194433
18	5	2	18.44571	18.45482	0.929320
19	2	5	18.44571	18.45482	0.369275
20	4	4	19.25249	19.27030	0.707107
21	5	3	19.81907	19.81831	0.858388
22	3	5	19.81907	19.84693	0.513001
23	6	1	20.67076	20.67252	0.986598
24	1	6	20.67076	20.67252	0.163171
25	6	2	21.40725	21.40620	0.949272
26	2	6	21.40725	21.41998	0.314456
27	5	4	21.60122	21.61612	0.781378
28	4	5	21.60122	21.61612	0.624058
29	6	3	22.58736	22.59719	0.895210
30	3	6	22.58736	22.59719	0.445645
31	5	5	23.69538	23.70905	0.707107
32	7	1	23.77804	23.77776	0.990082
33	1	7	23.77804	23.78119	0.140491
34	6	4	24.14838	24.14794	0.832716
35	4	6	24.14838	24.17276	0.553700
36	7	2	24.41650	24.42048	0.961940
37	2	7	24.41650	24.42048	0.273261
38	7	3	25.44889	25.44802	0.919778
39	3	7	25.44889	25.46396	0.392440
40	5	6	26.02045	26.03281	0.639759
41	6	5	26.02045	26.03281	0.768575
42	7	4	26.83209	26.84142	0.868900
43	4	7	26.83209	26.84142	0.494987
44	8	1	26.89357	26.90284	0.992368
45	1	8	26.89357	26.90284	0.123308
46	8	2	27.45680	27.46384	0.970443
47	2	8	27.45680	27.47055	0.241330

TABLE 3
(continued)

#	(l, m)		W	$L\tau$	η_1
48	6	6	28.13826	28.15015	0.707107
49	8	3	28.37326	28.38524	0.936829
50	3	8	28.37326	28.38524	0.349789
51	7	5	28.51523	28.51498	0.814239
52	5	7	28.51523	28.53654	0.580530
53	8	4	29.61210	29.61719	0.895014
54	4	8	29.61210	29.63325	0.446038
55	9	1	30.01470	30.03871	0.993948
56	1	9	30.01470	30.04016	0.109849
57	6	7	30.44707	30.45738	0.650488
58	7	6	30.44707	30.45738	0.759516
59	9	2	30.51843	30.54346	0.976410
60	2	9	30.51843	30.54348	0.215927
61	8	5	31.13563	31.14924	0.848538
62	5	8	31.13563	31.14925	0.529134
63	9	3	31.34175	31.36179	0.949076
64	3	9	31.34175	31.37103	0.315046
65	9	4	32.46189	32.48609	0.914314
66	4	9	32.46189	32.48609	0.405006
67	7	7	32.58114	32.59134	0.707107
68	8	6	32.90378	32.90756	0.800393
69	6	8	32.90378	32.92640	0.599476
70	10	1	33.13981	33.65843	0.995085
71	1	10	33.13981	33.65845	0.099028
72	2	10	33.59532	33.86583	0.195272
73	10	2	33.59532	33.88123	0.980749
74	9	5	33.85029	34.09484	0.874674
75	5	9	33.85029	34.09949	0.484712
76	10	3	34.34231	34.81780	0.958137
77	3	10	34.34231	34.81782	0.286309
78	7	8	34.87810	34.89094	0.658278
79	8	7	34.87810	34.89094	0.752775
80	10	4	35.36352	35.49740	0.928899
81	4	10	35.36352	35.49744	0.370333
82	9	6	35.47550	35.80116	0.832494
83	6	9	35.47550	35.81392	0.554034
84	11	1	36.26783	37.03777	0.995929
85	1	11	36.26783	37.04559	0.090139
86	10	5	36.63688	37.04562	0.894897
87	5	10	36.63688	37.14375	0.446273
88	11	2	36.68350	37.14472	0.984000
89	2	11	36.68350	37.31760	0.178168
90	8	8	37.02402	37.33437	0.707107
91	9	7	37.30595	37.53751	0.789665
92	7	9	37.30595	37.53752	0.613539
93	11	3	37.36689	38.18219	0.965012
94	3	11	37.36689	38.18976	0.262204
95	10	6	38.13743	38.50124	0.857940
96	6	10	38.13743	38.51931	0.513750
97	11	4	38.30459	39.07907	0.940146
98	4	11	38.30459	39.07908	0.340771
99	9	8	39.31195	39.33184	0.747565
100	8	9	39.31195	39.33184	0.664188

where a_0 is the *radius of the caustic*, and a is the radius of the circular plate. To find the additional *waves propagating (mainly) on the circumference* of the disk, we must find asymptotic solutions of (2.7) on Ω. However, for a circular domain, we can take advantage of the solution representation [7, p. 308]

$$\phi(r, \theta) = [a_1 J_n(kr) + a_2 J_n(ikr)]\, e^{\pm in\theta}, \quad k^2 = \lambda \quad \text{in (1.1)},$$

J_n: the Bessel function of order n

and recognize that the first two waves $J_n(kr)\, e^{\pm in\theta}$ are regular membrane-type waves; therefore the second two waves $J_n(ikr)\, e^{\pm in\theta}$ should be of the type of boundary waves that we are seeking. Therefore this suggests that the boundary waves on $\partial\Omega$ should have phase functions

$$S_j(ir, \theta), \qquad j = 1, 2.$$

For example,

$$S_1(ir, \theta) = a_0\left[\theta - \cos^{-1}\left(\frac{a_0}{ir}\right)\right] + (-r^2 - a_0^2)^{1/2}$$

$$= a_0\left[\theta \pm i \cosh^{-1}\left(\frac{r^2 + a_0^2}{r^2}\right)^{1/2}\right] \pm i(r^2 + a_0^2)^{1/2} + \text{const.}$$

The way in which the "$\pm$" signs are chosen in the above is difficult to decide. According to our a posteriori *analysis*, we should choose

$$S_1(ir, \theta) = a_0\left[\theta + i \cosh^{-1}\left(\frac{r^2 + a_0^2}{r^2}\right)^{1/2}\right] - i(r^2 + a_0^2)^{1/2}$$

(where the constant part is neglected). Thus

$$\exp[ikS_1(ir, \theta]) = \exp\left\{ika_0\theta + k\left[-a_0 \cosh^{-1}\left(\frac{r^2 + a_0^2}{r^2}\right)^{1/2} + (r^2 + a_0^2)^{1/2}\right]\right\},$$

good for $k < 0$ (in order for it to decay exponentially in the internal radial direction), and the leading term of the boundary wave propagating in the counterclockwise sense is

$$(5.1)\quad B(r, \theta) \exp\left(ika_0\theta + k\left[-a_0 \cosh^{-1}\left(\frac{r^2 + a_0^2}{r^2}\right)^{1/2} + (r^2 + a_0^2)^{1/2}\right]\right), \qquad k < 0,$$

as depicted in Fig. 6(a), where $B(r, \theta)$ is the (dominant) amplitude of the boundary

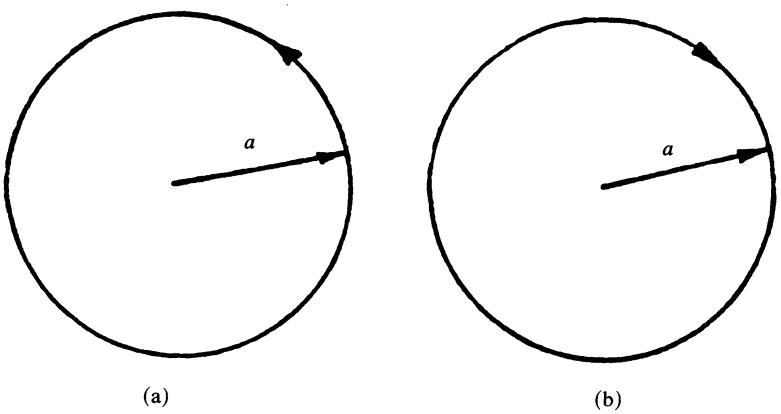

FIG. 6. *Two waves propagating mainly on the circumferences.*

wave. The second boundary wave propagating in the clockwise sense is then naturally

$$(5.1)' \quad B'(r,\theta)\exp\left(ika_0\theta - k\left[-a_0\cosh^{-1}\left(\frac{r^2+a_0^2}{r^2}\right)^{1/2}+(r^2+a_0^2)^{1/2}\right]\right), \qquad k>0$$

(see Fig. 6(b)). (As a matter of fact, the phase of the wave (5.1)′ corresponds to $ik\cdot S_2(ir,\theta)$.) Now consider $k<0$. The waves propagating on $\bar{\Omega}$ outside the caustic are

$$\begin{aligned}\phi(r,\theta) &= \sum_{j=1}^{2} e^{ikS_j(r,\theta)}\left[A_{j,0}(r,\theta)+\mathcal{O}\left(\frac{1}{k}\right)\right] \\ &\quad +\exp\left(ika_0\theta+k\left[-a_0\cosh^{-1}\left(\frac{r^2+a_0^2}{r^2}\right)^{1/2}+(r^2+a_0^2)^{1/2}\right]\right) \\ &\quad \cdot\left[B(r,\theta)+\mathcal{O}\left(\frac{1}{k}\right)\right].\end{aligned} \tag{5.2}$$

Applying the clamped boundary conditions

$$\phi(a,\theta)=0, \frac{\partial}{\partial r}\phi(r,\theta)|_{r=a}=0$$

to (5.2) and setting the dominant terms (i.e., those with the highest power of k) to zero, noting that

$$\frac{\partial}{\partial r}S_1(r,\theta)|_{r=a}=\frac{\sqrt{a^2-a_0^2}}{a}, \qquad \frac{\partial}{\partial r}S_2(r,\theta)|_{r=a}=-\frac{\sqrt{a^2-a_0^2}}{a},$$

$$\frac{\partial}{\partial r}\left\{ika_0\theta+k\left[-a_0\cosh^{-1}\left(\frac{r^2+a_0^2}{r^2}\right)^{1/2}+(r^2+a_0^2)^{1/2}\right]\right\}\Big|_{r=a}=\frac{\sqrt{a^2+a_0^2}}{a},$$

we get

$$\begin{aligned}&A_{1,0}(a,\theta)+B(a,\theta)\exp\left(a_0k\left[i\cos^{-1}\left(\frac{a_0}{a}\right)-\cosh^{-1}\left(\frac{a^2+a_0^2}{a^2}\right)^{1/2}\right]\right. \\ &\left.+k[(a^2+a_0^2)^{1/2}-i(a^2-a_0^2)^{1/2}]\right)+A_{2,0}(a,\theta)=0,\end{aligned} \tag{5.3}$$

$$\begin{aligned}&\frac{\sqrt{a^2-a_0^2}}{a}A_{1,0}(a,\theta)-i\frac{\sqrt{a^2+a_0^2}}{a}B(a,\theta) \\ &\cdot\exp\left(a_0k\left[i\cos^{-1}\left(\frac{a_0}{a}\right)-\cosh^{-1}\left(\frac{a^2+a_0^2}{a^2}\right)^{1/2}\right]+k[(a^2+a_0^2)^{1/2}-i(a^2-a_0^2)^{1/2}]\right) \\ &-\frac{\sqrt{a^2-a_0^2}}{a}A_{2,0}(a,\theta)=0.\end{aligned} \tag{5.4}$$

Multiplying (5.3) by $i\sqrt{a^2+a_0^2}/a$ and adding (5.4), we have eliminated $B(a,\theta)$ and obtained the reflection relation

$$A_{2,0}(a,\theta)=\frac{\sqrt{a^2-a_0^2}+i\sqrt{a^2+a_0^2}}{\sqrt{a^2-a_0^2}-i\sqrt{a^2+a_0^2}}A_{1,0}(a,\theta), \qquad 0\leqq\theta\leqq 2\pi.$$

Therefore the change of phase due to reflection for the clamped boundary conditions is

$$\delta(\arg A)=\arg\left(\frac{\sqrt{a^2-a_0^2}+i\sqrt{a^2+a_0^2}}{\sqrt{a^2-a_0^2}-i\sqrt{a^2+a_0^2}}\right)=-\pi-\cos^{-1}\left(\frac{a_0^2}{a^2}\right). \tag{5.5}$$

If $k>0$, we choose (5.1)′ and reverse the roles of the incident and reflected waves in (5.2)-(5.5). This will lead to the same relation (5.5). The covering space for the circular membrane wave propagation was recognized to be a *torus* in [11]. Here we again assume that the covering space for the circular plate wave propagation is also a torus. The two linearly independent paths C_1 and C_2 in the fundamental group of the torus are chosen as in Fig. 5 of [11]. (cf. Fig. 7). Using C_1 in (2.5), we get, as in [11, p. 33, (24)]

$$\oint_{C_1} \nabla S \cdot d\sigma = \text{arclength of } C_1 = 2\left(\sqrt{a^2-a_0^2} - a_0 \cos^{-1}\frac{a_0}{a}\right).$$

From (5.5) and the fact that the path C_1 has passed the caustic once with change of phase of amplitude $-\pi/2$ (cf. [11, p. 33, second and third lines from bottom]), we have

$$\sum \delta(\arg A) = -\pi - \cos^{-1}\left(\frac{a_0^2}{a^2}\right) - \frac{\pi}{2} = -\left[\frac{3}{2}\pi + \cos^{-1}\left(\frac{a_0^2}{a^2}\right)\right],$$

so (2.5) yields

$$(5.6)\quad k\left(\sqrt{a^2-a_0^2} - a_0 \cos^{-1}\frac{a_0}{a}\right) = \pi\left[m + \frac{3}{4} + \frac{1}{2}\cos^{-1}\left(\frac{a_0^2}{a^2}\right)\right], \qquad m = 0, 1, 2, \cdots.$$

Using C_2 in (2.5), we get

$$\oint_{C_2} \nabla S \cdot d\sigma = \text{arclength of } C_2 = 2\pi a_0,$$

so (2.5) gives

$$(5.7)\qquad k(2\pi a_0) = 2\pi l, \qquad l = 0, 1, 2, \cdots.$$

(Any unfamiliar reader can refer to [11, p. 33] for some comparison.) Eliminating a_0 in(5.6) from (5.7), we can solve for the wavenumber k. For $a=1$, the case of the unit circular plate, we have computed a few values of k from (5.6) and (5.7) (see the right half of Table 4) that agree closely with the (exact) values computed from [7, p. 308], tabulated on the left half of Table 4. This again demonstrates the success of the wave method for the thin plate equation.

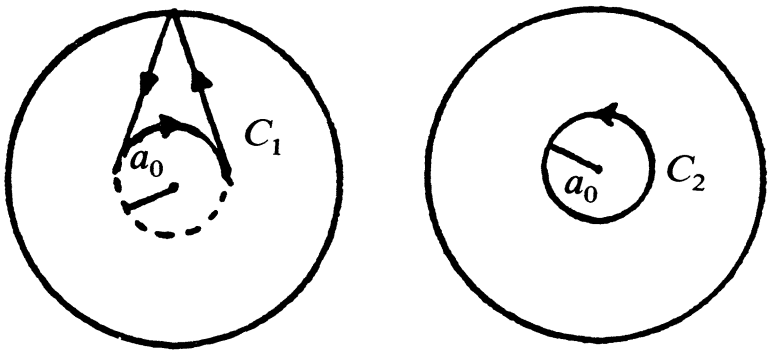

FIG. 7. *The two linearly independent paths C_1 and C_2 on the toroidal covering space for plate wave propagation.*

TABLE 4
Comparison of k, the wavenumber of a clamped unit circular plate.

#	Exact values computed from [7, p. 308]	(*l*, *m*)	Values computed by the wave method (5.6), (5.7)
1	3.19622	0, 0	3.141593
2	4.61090	1, 0	4.578895
3	5.90568	2, 0	5.881818
4	6.30644	0, 1	6.283185
5	7.14353	3, 0	7.123206
6	7.79927	1, 1	7.781379
7	8.34661	4, 0	8.237848
8	9.19688	2, 1	9.182366
9	9.43950	0, 2	9.424778
10	9.52570	5, 0	9.570534

REFERENCES

[1] L. BAUER AND E. L. REISS, *Block five diagonal matrices and the fast numerical solution of the biharmonic equation*, Math. Comp., 26 (1972), pp. 311-326.

[2] V. V. BOLOTIN, *An asymptotic method for the study of the problem of eigenvalues for rectangular regions*, in Problems of Continuum Mechanics, J. R. M. Radds, ed., Society for Industrial and Applied Mathematics, Philadelphia, PA, 1961, pp. 56-68.

[3] G. CHEN AND J. ZHOU, *The wave propagation method for the analysis of boundary stabilization in vibrating structures*, SIAM J. Appl. Math., 50 (1990), pp. 1254-1283.

[4] J. K. COHEN AND R. M. LEWIS, *A ray method for the asymptotic solution of the diffusion equation*, J. Inst. Math. Appl., 3 (1967), pp. 266-290.

[5] J. K. COHEN, F. G. HAGIN, AND J. B. KELLER, *Short time asymptotic expansion of solutions of parabolic equations*, J. Math. Anal. Appl., 38 (1972), pp. 82-91.

[6] M. P. COLEMAN, *The eigenfrequencies of a vibrating plate*, Ph.D. dissertation, Department of Mathematics, Pennsylvania State University, University Park, PA, December 1988.

[7] R. COURANT AND D. HILBERT, *Methods of Mathematical Physics*, Vol. I, Wiley-Interscience, New York, 1962.

[8] J. B. DELOS, *Semiclassical calculation of quantum mechanical wave functions*, in Advances in Chemical Physics, Vol. 55, I. Prigogine et al., ed., John Wiley, New York, 1986, pp. 161-214.

[9] D. GOTTLIEB AND S. ORSZAG, *Numerical Analysis of Spectral Methods, Theory and Applications*, Society for Industrial and Applied Mathematics, Philadelphia, PA, 1977.

[10] W. HACKBUSCH AND G. HOFMANN, *Results of the eigenvalue problem for the plate equation*, Z. Angew. Math. Phys., 31 (1980), pp. 730-739.

[11] J. B. KELLER AND S. I. RUBINOW, *Asymptotic solution of eigenvalue problems*, Ann. Physics, 9 (1960), pp. 24-75.

[12] J. B. KELLER, R. M. LEWIS, AND B. D. SECKLER, *Asymptotic solutions of some diffraction problems*, Comm. Pure Appl. Math., 9 (1956), pp. 207-265.

[13] J. B. KELLER, *A geometrical theory of diffraction*, in Proc. Symposia in Applied Mathematics, Vol. VII, McGraw-Hill, New York, 1958, pp. 27-52.

[14] G. KIRCHHOFF, *Über das Gleichgewicht und die Bewegung einer elastischene Scheibe*, J. Reine Angew. Math., 40 (1850), pp. 51-58.

[15] V. P. MASLOV AND M. V. FEDORIUK, *Semiclassical Approximation in Quantum Mechanics*, Reidel, Boston, 1981.